

EXIT Convergence Analysis of BICM-ID Based on High-Dimensional Modulation and Polar-TPC

Koike-Akino, T.; Wang, Y.; Kojima, K.; Millar, D.S.; Parsons, K.

TR2018-148 September 26, 2018

Abstract

We analyze polar turbo product codes (TPC) used with high-dimensional modulations (HDM). Our analysis reveals that the polar-TPC can significantly improve performance via iterative HDM demodulation employed across parallel and pipeline TPC decoding, achieving 2 dB gain for 16 dimensions.

European Conference on Optical Communication (ECOC)

This work may not be copied or reproduced in whole or in part for any commercial purpose. Permission to copy in whole or in part without payment of fee is granted for nonprofit educational and research purposes provided that all such whole or partial copies include the following: a notice that such copying is by permission of Mitsubishi Electric Research Laboratories, Inc.; an acknowledgment of the authors and individual contributions to the work; and all applicable portions of the copyright notice. Copying, reproduction, or republishing for any other purpose shall require a license with payment of fee to Mitsubishi Electric Research Laboratories, Inc. All rights reserved.

EXIT Convergence Analysis of BICM-ID Based on High-Dimensional Modulation and Polar-TPC

Toshiaki Koike-Akino, Ye Wang, Keisuke Kojima, David S. Millar, Kieran Parsons

Mitsubishi Electric Research Laboratories (MERL), Cambridge, MA 02139, USA.

koike@merl.com

Abstract We analyze polar turbo product codes (TPC) used with high-dimensional modulations (HDM). Our analysis reveals that the polar-TPC can significantly improve performance via iterative HDM demodulation employed across parallel and pipeline TPC decoding, achieving 2 dB gain for 16 dimensions.

Introduction

A great amount of efforts in developing high-gain forward error correction (FEC) codes has been put forward next-generation optical communications, e.g., low-density parity-check (LDPC) codes^{1,2}, staircase codes^{3,4}, turbo product codes (TPC)⁵⁻⁷, and polar codes⁷⁻⁹. Recently, polar codes have drawn much attention since they were selected in wireless 5G standard because of the competitive performance (approaching the Polyanskiy bound) against state-of-the-art LDPC codes, thanks to successive cancellation list (SCL) decoding⁸. Nevertheless, one major drawback of polar SCL decoding lies in the difficulty of parallel implementation, leading to low throughput. To tackle this issue, we have proposed polar-TPC⁷ which constitutes spatially-coupled parallel short-block polar codes, rather than uncoupled long polar code. With parallel and pipeline SCL decoding, the proposed polar-TPC $(256, 239)^2$ achieves roughly 256-times faster decoding throughput. In addition, the use of irregular polarization⁹ reduces the decoding power by 72% and latency by 88%. The polar-TPC offers 0.5 dB gain over the conventional TPC based on Bose–Chaudhuri–Hocquenghem (BCH) codes.

In this paper, we further investigate polar-TPC in the context of bit-interleaved coded modulation with iterative demodulation (BICM-ID). Although BICM-ID is known to improve performance compared to BICM in particular for high-order modulation, the stand-alone polar codes were not suited for BICM-ID because of the successive decoding nature of the SCL algorithm. In contrast, the polar-TPC is suitable for BICM-ID because the intermediate decoding feedback is readily available for demodulation along turbo iterations over parallel SCL decoding. We analyze the performance benefit of polar-TPC for BICM-ID systems. Specifically, we focus on various high-dimensional modulations (HDM)¹⁰⁻¹⁴. HDM has

also received much interest in optical research community because of its high sensitivity. With the extrinsic information transfer (EXIT) chart, we study the convergence behavior of BICM-ID based on polar-TPC and HDM. Our analysis shows that higher dimension offers significant improvement by 2 dB when BICM-ID was employed for few-iteration polar-TPC decoding.

Polar turbo product codes (Polar-TPC)

The polar SCL decoding has log-linear complexity of $\mathcal{O}[N \log(N)]$, which can be a drawback compared to linear-complexity belief-propagation (BP) decoding of LDPC codes. However, the non-linear complexity turns to be advantageous when we shorten the block length N . Fig. 1 illustrates the complexity analysis (the required number of additions at variable nodes) of polar SCL decoding and LDPC BP decoding. It suggests that the polar codes can be simpler than most irregular LDPC codes when the block size is smaller than 5000 bits. Note that irregular polar codes⁹ can further reduce the computational complexity by 50–70%. Suggested by the nonlinear complexity, short-length polar codes shall be used in parallel to construct long codes via spatial coupling. The polar-TPC is one of such approaches.

Fig. 2 illustrates TPC $(N, k)^2$ using multiple polar constituent codes, instead of BCH. For the two-dimensional architecture, the TPC performs two-stage encoding, i.e., column- and row-encoding over a $k \times k$ information block, to generate an $N \times N$ encoded block. We can implement a highly parallel encoder, i.e., k -parallel column encoding followed by N -parallel row encoding. Each polar code (N, k) performs n -stage polarization steps ($n = \log_2 N$) with pre-defined $(N - k)$ -bit frozen insertion and irregular polar pruning⁹.

The TPC decoder performs row- and column-decoding iteratively via turbo Chase processing. Since the decoding can be performed in a fully parallel fashion for N component codes inde-

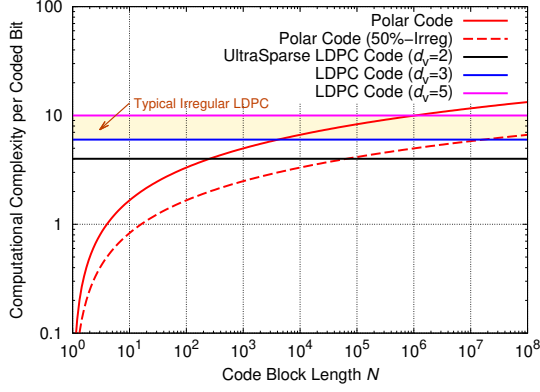


Fig. 1: Per-bit computational complexity of LDPC decoding and polar decoding over different block lengths.

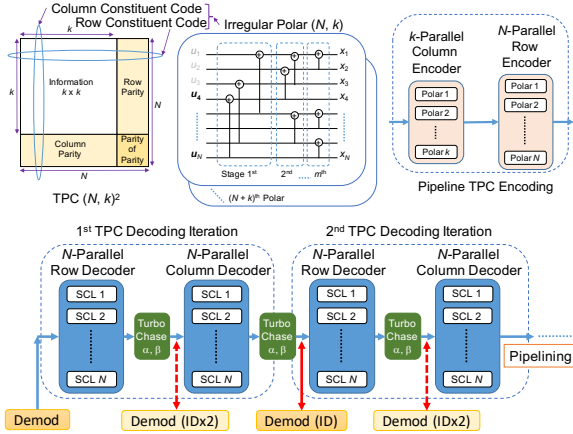


Fig. 2: Polar-TPC $(N, k)^2$, capable of highly parallel and pipeline SCL decoding with iterative demodulation (ID).

pendently (and pipelines across turbo iterations), the TPC enables roughly N -times higher decoding throughput compared to a single uncoupled N^2 -length polar code. Note that SCL algorithm is suited for Chase processing because multiple candidates are obtained without modifications.

Fig. 3 shows the benefit of polar-TPC in terms of bit-error-rate (BER) performance for quadrature phase-shift keying (QPSK). We consider $I = 4$ iterations for polar-TPC $(256, 239)^2$ (irregular 50%) with a list size of $L = 16$, and BCH-TPC $(256, 239)^2$ with Berlekamp–Massey (BM) 32-pattern Chase decoding. We also present the performance of SCL decoding ($L = 32$) for a long polar code $(256^2, 239^2 + 16)$, concatenated with cyclic redundancy check (CRC) 16 bits. It is seen that the BER of the polar-TPC approaches that of the long polar code within 0.2 dB after four iterations, even though the decoding throughput can be 256-times faster in principle. Moreover, it is verified that the polar-TPC outperforms the conventional BCH-TPC by 0.5 dB. We also confirm that 60-iteration BP decoding for polar-TPC does not compete with SCL Chase decoding.

When higher-order modulation is used, the

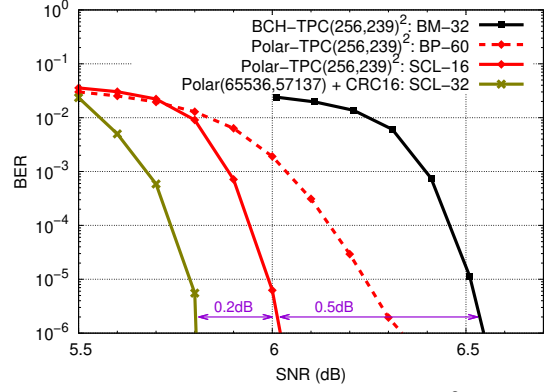


Fig. 3: Polar-TPC vs. BCH-TPC for $(256, 239)^2$ with $I = 4$ turbo iterations for QPSK.

polar-TPC may be further improved by BICM-ID, where demodulator output is refined by exploiting intermediate decoding messages after each iteration as shown in Fig. 2. We can also update demodulator output twice per iteration between row and column decoding (denoted by ‘IDx2’).

High-dimensional modulation (HDM)

We analyze BICM-ID employing HDM^{10–14}, which provides larger Euclidean distance to be robust against noise. There are many ways to design HDM formats such as lattice cutting and block coding¹². Fig. 4 compares different HDM schemes in terms of spectral efficiency vs. sensitivity (proportional to minimum squared Euclidean distance). It is shown that higher dimension offers significant improvement in sensitivity; specifically, 24-dimensional modulation achieves 6 dB gain. Although lattice cutting is mostly better than block coding, it suffers from labeling issue, leading to lower generalized mutual information. Hence, this paper focuses on more practical block-coded HDM. Note that 16-dimensional HDM¹⁴ based on the nonlinear Nordstrom–Robinson (NR) code achieves 0.5 and 0.8 dB gains over the lattice cut and best-known linear code (BKLC), respectively.

Nonetheless, the sensitivity gain is only visible at the very high signal-to-noise ratio (SNR) regimes, where error events are dominated by minimum distance pairs. In fact, more notable benefit of HDM schemes will appear when BICM-ID is employed. This is illustrated in Fig. 5, which shows EXIT curves of HDM demodulator given feedback from decoder ends. With the increased HDM dimensionality, more steep EXIT curves can be seen. Therefore, slight increase of *a priori* mutual information given FEC feedback can provide much more reliable demodulator output to the FEC decoder. Whereas, the 24-dimensional demodulator has only a little gain to increase the

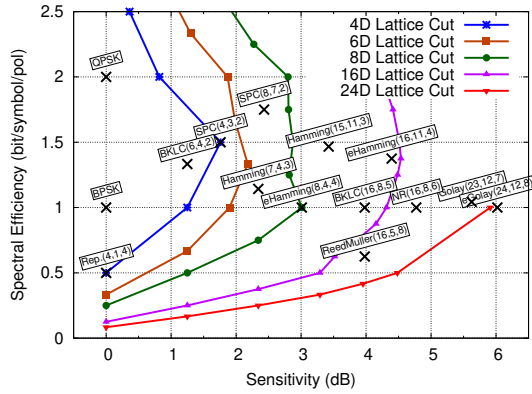


Fig. 4: Sensitivity of various HDM schemes¹².

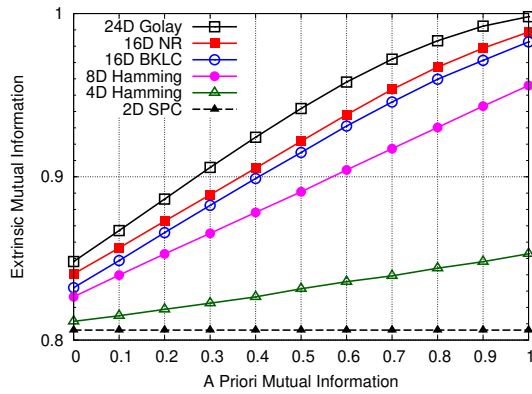


Fig. 5: EXIT chart of HDM demodulator (1 dB SNR).

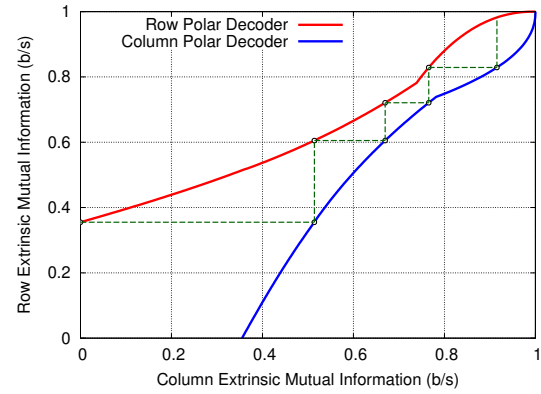


Fig. 6: EXIT chart of polar-TPC decoder (5.5 dB SNR).

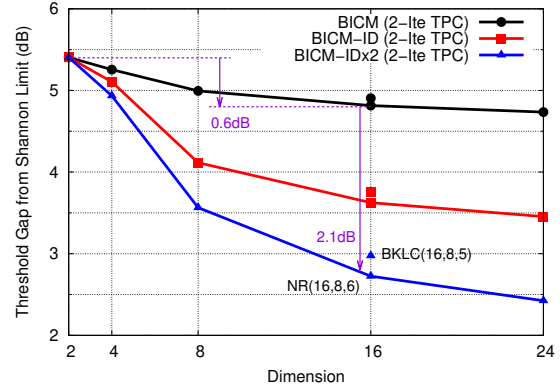


Fig. 7: Threshold of polar-TPC HDM with/without iterative demodulation (2-iteration TPC decoding).

mutual information if there is no decoder feedback, i.e., at *a priori* mutual information of zero.

BICM-ID with polar-TPC and HDM

Fig. 6 shows the EXIT chart of polar-TPC decoder with SCL Chase decoding ($L = 16$). The analysis shows that the TPC achieves error free after many iterations at an SNR of 5.5 dB. However, in practice, we should consider the FEC threshold at finite iterations. Using EXIT curves of both polar-TPC (Fig. 6) and HDM (Fig. 5), we can analyze the FEC threshold with and without ID as shown in Fig. 7, where the threshold after 2-iteration decoding is present across HDM dimension. As discussed, higher dimension provides marginal gain for BICM systems, e.g., 0.6 dB gain for 16-dimension HDM. In contrast, additional 2 dB gain is achievable by BICM-ID systems.

Conclusions

We study BICM-ID with polar-TPC and HDM. It was shown that polar-TPC can achieve significant performance gain greater than 2 dB via iterative demodulation for 16-dimensional HDM.

References

[1] I. B. Djordjevic, "Advanced coded-modulation for ultra-high-speed optical transmission," *OFC* (2014): W3J-4.
 [2] L. Schmalen, V. Aref, J. Cho, D. Suikat, D. Rösener, A. Leven,

"Spatially coupled soft-decision error correction for future light-wave systems," *JLT* **33** 5 (2015): 1109–1116.

- [3] B. P. Smith, A. Farhood, A. Hunt, F. R. Kschischang, J. Lodge, "Staircase codes: FEC for 100 Gb/s OTN," *JLT* **30** 1 (2012): 110–7.
 [4] C. Fougstedt, P. Larsson-Edefors, "Energy-efficient high-throughput staircase decoders," *OFC* (2018): Tu3C-6.
 [5] F. Paludi et al., "Low-complexity turbo product code for high-speed fiber-optic systems based on expurgated BCH codes," *IEEE ISCAS* (2016): 429–32.
 [6] S. Dave et al., "Soft-decision forward error correction in a 40-nm ASIC for 100-Gbps OTN applications," *OFC* (2011): JWA014.
 [7] T. Koike-Akino et al., "Irregular polar turbo product coding for high-throughput optical interface," *OFC* (2018): Tu3C.5.
 [8] B. Li, H. Shen, D. Tse, "An adaptive successive cancellation list decoder for polar codes with cyclic redundancy check," *IEEE COMM L* **16** 12 (2012): 2044–47.
 [9] T. Koike-Akino et al., "Irregular polar coding for complexity-constrained lightwave systems," *JLT* **36** 11 (2018): 2248–58.
 [10] E. Agrell, M. Karlsson, "Power-efficient modulation formats in coherent transmission systems," *JLT* **27** 22 (2009): 5115–26.
 [11] T. Liu, I. B. Djordjevic, "Multidimensional optimal signal constellation sets and symbol mappings for block-interleaved coded-modulation enabling ultrahigh-speed optical transport," *IEEE Photon. J.* **6** 4 (2014): 1–14.
 [12] D. S. Millar et al., "High-dimensional modulation for coherent optical communications systems," *Opt. Exp.* **22** 7 (2014): 8798–812.
 [13] A. D. Shiner et al., "Demonstration of an 8-dimensional modulation format with reduced inter-channel nonlinearities in a polarization multiplexed coherent system," *Opt. Exp.* **22** 17 (2014): 20366–74.
 [14] T. Koike-Akino et al., "LDPC-coded 16-dimensional modulation based on the Nordstrom–Robinson nonlinear block code," *CLEO* (2015): JTh2A.59.